A New Approach for the Synthesis of Au−Ag Alloy Nanoparticle Incorporated SiO_2 Films

Sudipto Pal and Goutam De*

Sol-Gel Division, Central Glass and Ceramic Research Institute, 196, Raja S. C. Mullick Road, Jadavpur, Kolkata 700 032, India

Received July 19, 2005. Revised Manuscript Received September 27, 2005

A new synthesis procedure has been developed to prepare Au−Ag alloy nanoparticles inside glassy SiO_2 film matrix. Two successive overlapping coating layers were prepared on glass substrate using Au- and Ag-incorporated inorganic−organic hybrid silica sols, respectively. The concentrations of the Au and Ag (3 equivalent mol % metal − 97% silica in each case) in the respective layers and their individual coating thicknesses were kept similar for the generation of 1:1 Au−Ag ($Au_{0.5}Ag_{0.5}$) alloy. The dried two-layer (TL) coating assembly after UV (2.75 J/cm^2) and followed by thermal treatments (450−550 °C) yielded Au−Ag alloy nanoparticles of controllable molar ratios in a glassy SiO_2 matrix. Thus, the UV-treated TL film when heated at 450 °C yielded spherical Au−Ag alloy nanoparticles (Au mol fraction $\approx$ 0.8) of average diameter ($\langle D \rangle$) 2.5 nm whereas the 550 °C heated film sample showed relatively larger alloy nanoparticles of $\langle D \rangle$ 4.5 nm having Au mol fraction of $\approx$0.5. The alloy nanoparticles were formed through the interlayer diffusion of Ag and Au during the thermal annealing in the solid state.

Introduction

Noble metal nanoparticles (e.g., Au and Ag) with their associated strong surface plasmon resonance (SPR) have generated great interest in fields such as optical switching[1] and optical sensing.[2] In particular, when embedded in appropriate glassy hosts, the third-order susceptibility of nanometals at wavelengths around the SPR achieves large values with very fast (ps) response times.[1] There is considerable interest today in synthesizing gold−silver alloy nanoparticles from solution under different conditions.[3] All published literature showed a linear dependence of the SPR absorption maximum on the composition of the alloy nanoparticles having size ranges of about 5−30 nm.[3,4] For real applications, however, the nanocrystals have to be embedded in a suitable matrix which can withstand high-intensity laser light. We have shown that the sol−gel derived metal nanocrystals incorporated in SiO_2 films exhibit high $\chi^{(3)}$ values with good reproducibility.[1c,e] It is also noteworthy that we have successfully synthesized different binary alloy nanoparticle (e.g. Au−Cu,[5] Co−Ni,[6] and Au−Pt[7]) doped coatings from sols obtained by simply mixing soluble nitrate or chloride salts into TEOS-derived silica sols followed by thermal annealing. However, this simple approach failed in the case of the Au−Ag system because of nonavailability of Au- and Ag-salts remaining soluble in a common solvent.

In this paper, we report, for the first time, a new sol−gel approach for the preparation of Au−Ag alloy nanoparticles following deposition of two successive overlapping individual layers of Au- and Ag-doped sols respectively on glass substrates followed by UV treatment and thermal annealing. The alloy formation with tuneable Au/Ag compositional control has been accomplished in an amorphous glassy matrix through interlayer diffusion of Ag and Au nanoparticles in the solid state. Such alloy nanocrystals of very uniform size distributions, belonging to the quantum-size regime embedded in glassy SiO_2 film, expected to show interesting nonlinear optical responses.

Experimental Section

Preparation of Sols. All chemicals were used as received. Tetraethyl orthosilicate (TEOS) and 3-(glycidoxypropyl)trimethoxysilane (GLYMO) were supplied by Sigma-Aldrich, while $HAuCl_4$·

* Corresponding author. Fax: +91 33 24730957. E-mail: gde@cgcri.res.in.

(1) (a) Hache, H.; Ricard, D.; Flytzanis C. *J. Opt. Soc. Am.* **1986**, *B3*, 1647. (b) Flytzanis C.; Hache, F.; Klein, M. C.; Ricard, D.; Roussignol, Ph. *Prog. Opt.* **1991**, *29*, 321. (c) De, G.; Tapfer, L.; Catalano, M.; Battaglin, G.; Caccavale, F.; Gonella, F.; Mazzoldi, P.; Haglund, R. F., Jr. *Appl. Phys. Lett.* **1996**, *68*, 3820. (d) Sun, Y.-P.; Riggs, J. E.; Henbest, K. B.; Martin, R. B. *J. Nonlinear Opt. Phys. Mater.* **2000**, *9*, 481. (e) Prem Kiran, P.; Shivakiran Bhaktha, B. N.; Rao, D. N.; De, G. *J. Appl. Phys.* **2004**, *96*, 6717. (f) Wang, Q.; Wang, S.; Hang, W.; Gong, Q. *J. Phys. D: Appl. Phys.* **2005**, *38*, 389. (g) Yu, S. W.; Liao, H. B.; Wen, W. J.; Wong, G. K. L. *Opt. Mater.* **2005**, *27*, 1433.

(2) (a) Yonzon, C. R.; Jeoung, E.; Zou, S.; Schatz, G. C.; Mrksich, M.; Van Duyne, R. P. *J. Am. Chem. Soc.* **2004**, *126*, 12669. (b) Riboh, J. C.; Haes, A. J.; McFarland, A. D.; Yonzon, C. R.; Van Duyne, R. P. *J. Phys. Chem. B* **2003**, *107*, 1772. (c) Raschke, G.; Kowarik, S.; Franzl, T.; Sönnichsen, C.; Klar, T. A.; Feldmann, J.; Nichtl, A.; Kürzinger, K. *Nano Lett.* **2003**, *3*, 935. (d) McFarland, A. D.; Van Duyne, R. P. *Nano Lett.* **2003**, *3*, 1057.

(3) (a) Papavassiliou, G. C. *J. Phys. F: Met. Phys.* **1976**, *6*, L103. (b) Link, S.; Wang, Z. L.; El-Sayed, M. A. *J. Phys. Chem. B* **1999**, *103*, 3629. (c) Chen, Y.-H.; Yeh, C.-S. *Chem. Commun.* **2001**, 371. (d) Izgaliev, A. T.; Simakin, A. V.; Shafeev, G. A.; Bozon-Verduraz, F. *Chem. Phys. Lett.* **2004**, *390*, 467. (e) Liu, Y.-C.; Lee, H.-T.; Peng, H.-H. *Chem. Phys. Lett.* **2004**, *400*, 436. (f) Sun, Y.; Xia, Y. *Analyst* **2003**, *128*, 686.

(4) Lee, I.; Han, S. W.; Kim, K. *Chem. Commun.* **2001**, 1782.

(5) (a) De, G.; Mattei, G.; Mazzoldi, P.; Sada, C.; Battaglin, G.; Quaranta, A. *Chem. Mater.* **2000**, *12*, 2157. (b) De, G.; Rao, C. N. R. *J. Phys. Chem. B* **2003**, *107*, 13597.

(6) Mattei, G.; de Julián Fernández, C.; Mazzoldi, P.; Sada, C.; De, G.; Battaglin, G.; Sangregorio, C.; Gatteschi, D. *Chem. Mater.* **2002**, *14*, 3440.

(7) De, G.; Rao, C. N. R. *J. Mater. Chem.* **2005**, *15*, 891.

10.1021/cm051572r CCC: $30.25
Published on Web 11/02/2005

$3H_2O$, $AgNO_3$, *n*-butanol, and methanol were obtained from s.d. fine-chem limited. Aluminum acetylacetonate ($Al(acac)_3$) was supplied by Lancaster.

First, undoped inorganic−organic hybrid sols were prepared using TEOS, GLYMO, *n*-butanol, water, methanol, HCl or HNO_3, and $Al(acac)_3$. The last two chemicals were used in catalytic amount for alkoxide hydrolysis and epoxy polymerization initiator, respectively. Then 21.5 mmol of TEOS and 9.2 mmol of GLYMO were dissolved in *n*-butanol (65 wt % of total). To this, a mixture of acid (HCl or HNO_3; 5×10^{-4} mol/mol of alkoxy group), water (0.5 mol/mol of alkoxy group), and methanol was added to the above solution with stirring. The stirring was continued for 30 min and the resultant mixture was refluxed for 60 min to obtain a hybrid sol. A catalytic amount of $Al(acac)_3$ (0.05 mol/mol of GLYMO) was added at this stage, stirring until it dissolved, followed by the remaining amount of *n*-butanol (35%) and stirring was continued for another 30 min. The resulting clear sol was then used for doping. The HNO_3 and HCl catalyzed sols are used for Ag and Au doping, respectively. The molar ratio of the Ag or Au metal to the SiO_2 was kept constant in the sols, being 3 equivalent mol % Au or Ag − 97% SiO_2. The calculated amount of $HAuCl_4 \cdot 3H_2O$ or $AgNO_3$ was dissolved in a small amount of water (molar ratio of water to $HAuCl_4 \cdot 3H_2O$ and $AgNO_3$ can be varied from 10 to 12 and 26−28, respectively) and added to the corresponding undoped sols with stirring. In the final coating sol, about 8 equivalent wt % of SiO_2 was maintained.

Preparation of Coatings. Prior to the coating deposition, the silica glass slides (Heraus, Suprasil 3; thickness 0.5 mm) were first cleaned with a warm neutral detergent solution, followed by rinsing with distilled water and 2-propanol, and finally, boiled in 2-propanol for 5 min. The coatings were prepared using the dipping technique (Dip-master 200, Chemat Corporation) with a withdrawal velocity of 2.5 in./min. First, Au-doped coating was deposited on a cleaned substrate and dried at 60 °C for 30 min followed by a second coating being applied onto it using Ag-doped sol. The two-layer (designated as TL) coating assembly was again dried at 60 °C for 30 min followed by UV treatment (2.75 J/cm^2) using a conveyorized UV curing machine. The UV energy was monitored using a UV intensity meter (UV Power Puck, EIT). This UV-treated TL coating was then heated at 450, 500, and 550 °C in air in cumulative heating procedures. Similar coatings were deposited on silicon wafers (intrinsic, IR transparent) for the IR spectral studies.

The thickness of the coatings was measured by a Surfcorder SE-2300 profilometer (Kosaka Laboratory Ltd., Japan). Infrared absorption spectra of the films deposited on silicon wafers were recorded by FTIR spectrometry (Nicolet, model 5PC) with a resolution of 4 cm^{-1} and 500 scans for each sample. The UV−visible spectra of the coatings deposited on silica glass substrates were obtained using a Cary 50 scan spectrophotometer. Powder X-ray diffraction (XRD) patterns of the coatings deposited on silica glass substrates were recorded with a diffractometer, operating at 40 kV and 30 mA using Ni-filtered Cu Kα radiation. Transmission electron microscopic (TEM) measurements were carried out with a JEOL 2010 transmission electron microscope at IACS, Kolkata. TEM samples were prepared by scraping the heat-treated films deposited on silica glass substrate. The scraped films were first dispersed in methanol under ultrasonication, and one small drop of this dispersion was deposited onto a carbon-coated grid on an underlying tissue paper.

Results and Discussion

The TEOS-GLYMO combined approach is used here to prepare crack-free, relatively thicker, and porous coatings on glass substrates.[8] The matrix refractive index of the coatings after heat treatment at 500 °C is found to be 1.411 at 550 nm.[8] Table 1 shows the thickness evolution of the Au- and Ag-doped single-layer films with respect to the UV/thermal treatment temperatures. In the TL coatings, Au- and Ag-layers were prepared following identical conditions as those of single layers. The total thickness of the final heat-treated (550 °C/2 h) TL film was found to be 390 ± 10 nm. This thickness value matches well with the sum of thickness values of heat-treated (550 °C) single-layer Au- and Ag-doped films (Table 1). The concentrations of the Au and Ag (3 equivalent mol % metal − 97% silica in each case) in the respective layers and their individual coating thicknesses are kept similar keeping in view the formation of 1:1 Au−Ag alloy. The as-prepared, dried, and UV/thermal-treated films were visually clear, spot-free, and transparent. The adhesion and hardness of the heat-treated (450−550 °C) coatings were found to be excellent. The pencil hardness value (measured following the specifications of ASTM D 3363) of the heat-treated (450−550 °C) coatings is greater than 9H and no scratch mark on the coatings was observed after rubbing the coating surfaces with #000 grade steel wool. These results confirmed that the coatings are strongly adhering to the substrates and sufficiently hard to use for any practical purposes.

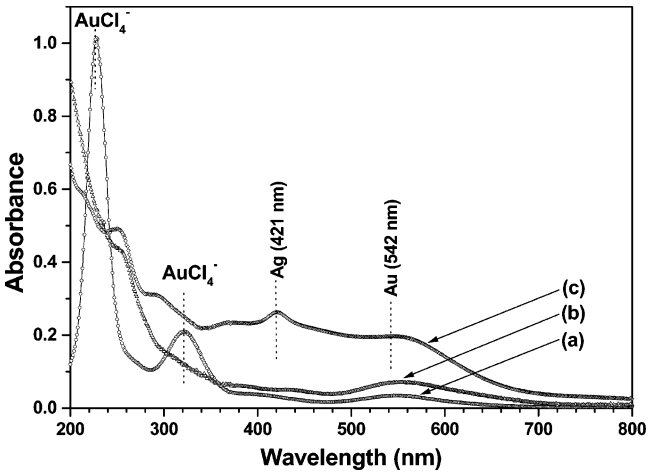

Figure 1. UV−visible spectra after deposition of (a) Au-doped film (first layer) dried at 60 °C, (b) Ag-doped film onto the first layer and dried at 60 °C, and (c) after UV treatment (2.75 J/cm^2) of the two-layer (TL) film assembly using a conveyorized UV-curing machine.

Table 1. Thickness Evolution of the Au- and Ag-Doped Films (Single Layer) with Respect to the UV and Heat Treatment Temperatures

	treatment (UV/ thermal)			
doped films	60 °C	UV (2.75 J/cm^2)	450 °C/1 h	550 °C/2 h
Au	340 ± 10 nm	310 ± 10 nm	240 ± 10 nm	210 ± 10 nm
Ag	340 ± 10 nm	280 ± 10 nm	210 ± 10 nm	190 ± 10 nm

3.1. Optical Absorption. Figure 1 shows the UV−visible spectral evolution after depositions of the first layer with Au-doped sol (Figure 1, curve a), followed by the second layer with Ag-doped sol on the first layer (Figure 1, curve b). Spectra were taken after drying the coating layers at 60 °C. Figure 1a shows the presence of a small broad Au-SPR peak at around 552 nm due to the formation of a small

(8) Medda, S. K.; De, S.; De, G. *J. Mater. Chem.* **2005**, *15*, 3278.

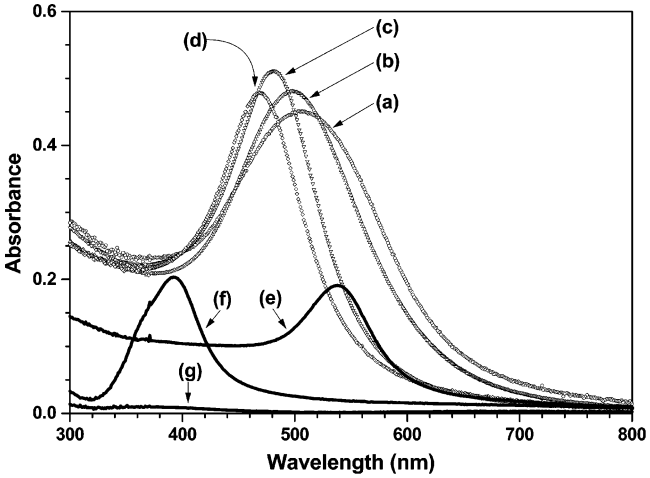

Figure 2. UV−visible spectral evolution of the UV-treated TL film after heat treatment at different temperatures in air: (a) 450 °C for 1 h, (b) 500 °C for 1 h, (c) 550 °C for 1 h, and (d) 550 °C for 2 h. The spectra of one-layer Au- and Ag-doped films heat-treated at 550 °C in air or H_2-N_2 atmosphere are also shown: (e) Au-doped film heated in air, (f) Ag-doped film heated in H_2-N_2, and (g) Ag-doped film heated in air.

amount of Au nanoparticles and strong peaks at 320 and 227 nm due to the charge transfer between the Au and chloro ligands of $AuCl_4^-$ ions.[9] After deposition of the second layer with Ag-sol, peaks at 320 and 227 nm disappeared (Figure 1, curve b), indicating decomposition of $AuCl_4^-$ ions. At this stage we can expect formation of some AgCl by reaction with $AuCl_4^-$ and $AgNO_3$. Figure 1b also shows more intensified broad Au-SPR peak at about 552 nm and a very weak peak around 430 nm due to Ag-SPR and, as a consequence, the dried TL films looked light bluish-pink in color. The film is then subjected to UV treatment to decompose Ag (including AgCl[10]) and remaining Au ions present in the film.[9,11] The UV-treated TL film shows clear peaks at about 542 and 421 nm (Figure 1, curve c) due to Au- and Ag-SPR absorptions, respectively. At this stage, the color of the film changes to purple with an orange hue. This composite TL film when heated in air at 450−550 °C shows a single and strong absorption peak (Figure 2, curves a−d) between the Ag- (∼395 nm) and Au-SPR (∼540 nm) positions (Figure 2, curves e and f), indicating formation of Au−Ag alloy.[3,4,12] The Au−Ag alloy formation is concluded from the fact that the optical absorption spectrum shows only one plasmon band.[3] Two plasmon bands would be expected for the case of a mixed (separate existence of Au and Ag) or core−shell type nanoparticles as observed by other workers[13,14] as well as in the UV-treated TL film (Figure 1, curve c).

It has been observed that the Au- and Ag-SPR peak intensities in the TL films after UV treatment are comparable (Figure 1, curve c) with those of one-layer Au- and Ag-doped films heated at 550 °C in air and 10% $H_2-90\%$ N_2 atmosphere respectively (Figure 2, curves e and f).[15] However, when the UV-treated TL film is heated at 450 °C or higher, the SPR peak intensity has been increased to more than double compared to Au- and Ag-SPR peak intensities as observed in the case of UV-treated film. After heating at 450 °C for 1 h, the TL film becomes red in color and as a consequence a strong absorption peak at 504 nm has been observed (Figure 2, curve a); this peak is gradually blue-shifted to 468 nm after annealing at 550 °C for 2 h (Figure 2, curves a−d). No further peak shifting upon increasing the holding time (≥3 h) at 550 °C has been observed; instead, we observe a slight decrease in intensity of the 468 nm peak.[16] The TL film after heat treatment at 550 °C/2 h was orange in color. Table 2 shows SPR peak positions and the corresponding full-width at half-maximum (fwhm) values with respect to the heat-treatment temperatures. The fwhm of the SPR peaks are gradually decreased with increasing temperature, indicating an increase in nanoparticles' size.[17] It may be noted here that the one-layer Au- or Ag-doped coatings showed clear Au- and Ag-SPR peaks at about 542 and 421 nm, respectively, after UV treatment. When these UV-treated single-layer films are heated in air at 550 °C, the characteristic Au-SPR peak has been retained at 542 nm (Figure 2, curve e); however, the Ag-SPR disappeared (Figure 2, curve g). The Ag-SPR reappeared with blue-shifting at 395 nm[1c] when the coating was reheated again at 400−550 °C in a reducing (10% $H_2-90\%$ N_2) atmosphere (Figure 2, curve f).[18] As air-annealed Ag-doped films are colorless, we did not observe any Ag-SPR peaks in cases of TL films heated at 450 °C and above where the unalloyed Ag fraction coexisted with the Au−Ag alloy nanoparticles (partially alloyed Ag with Au) in the film matrix. The appearance of Ag-SPR after UV curing and its disappearance after heat treatment in air suggests oxidation of Ag nanoparticles to lose the plasmon-based absorption band.[18] It has been pointed out earlier that we maintained same concentra-

Table 2. Evolution of SPR Absorptions with Respect to the UV and Thermal Treatments of the TL Film and Au−Ag Alloy Compositions Calculated from the Respective SPR Positions

treatment (UV/ thermal)	SPR peak position (nm)	fwhm (nm)	Au fraction (x_{Au}) calculated using ref 3f	Au:Ag molar ratio in the alloy
UV/2.75 J/cm^2	421, 542			
450 °C/1 h	504	169	0.81	4.3:1
500 °C/1 h	497	144	0.75	3:1
550 °C/1 h	480	100	0.60	1.5:1
550 °C/2 h	468	95	0.50	1:1

(9) (a) De, G.; Kundu, D. *Chem. Mater*. **2001**, *13*, 4239. (b) Torigoe, K.; Esumi, K. *J. Phys. Chem. B* **1999**, *203*, 2862.
(10) (a) Zayat, M.; Einot, D.; Reisfeld, R. *J. Sol-Gel Sci., Technol*. **1997**, *10*, 67. (b) Volkan, M.; Stokes, D. L.; Vo-Dinh, T. *Sens. Actuators B* **2005**, *106*, 667.
(11) De, G.; Kundu, D. *J. Non-Cryst. Solids* **2001**, *288*, 221.
(12) Padovani, S.; D'Acapito, F.; Cattaruzza, E.; De Lorenzi, A.; Gonella, F.; Mattei, G.; Maurizio, C.; Mazzoldi, P.; Montagna, M.; Ronchin, S.; Tosello, C.; Ferrai, M. *Eur. Phys. J. B* **2002**, *25*, 11.
(13) (a) Mulvaney, P. *Langmuir* **1996**, *12*, 788. (b) Mulvaney, P.; Giersig, M.; Henglein, A. *J. Phys. Chem*. **1993**, *97*, 7061.
(14) Kreibig, U.; Volmer, M. *Optical Properties of Metal Clusters*; Springer-Verlag: Berlin, 1995.

(15) In the case of UV-treated two-layer film the absorbance value of Ag-SPR (0.27) is higher than that of single-layer Ag-doped film (0.20). In the former case the higher absorbance value is due to the contribution of interband absorption of Au in the same wavelength region.
(16) We did not increase the heat-treatment temperature beyond 550 °C in air because above this temperature we observed loss of Ag from the coatings. See for example De, G.; Gusso, M.; Tapfer, L.; Catalano, M.; Gonella, F.; Mattei, G.; Mazzoldi, P.; Battaglin, G. *J. Appl. Phys.* **1996**, *80*, 6734.
(17) (a) Arnold, G. W. *J. Appl. Phys*. **1975**, *46*, 4466. (b) De, G. *J. Sol-Gel Sci. Technol*. **1998**, *11*, 289.
(18) This film when again heated in air became colorless. This bleaching and regaining of color is reversible upon heat treatment in air (oxidizing atmosphere) and H_2-N_2 (reducing atmosphere). The details will be published separately.

tions of Au and Ag in the sol as well as individual film thickness values so that the final alloy composition would be $Au_{0.5}Ag_{0.5}$ (Au:Ag = 1:1). From the SPR absorption peak position we have calculated the alloy composition based on the relationship between the SPR peak position and the molar fraction of Au (x_{Au}) as reported by Sun and Xia.[3f] Other published literature data also show more or less similar dependence between the Au−Ag alloy SPR peak position and the x_{Au} present in the alloy nanoparticles of different size (diameter) distributions prepared under different experimental conditions, e.g., 18 nm,[3b] 13.7 nm,[3c] 10 nm,[3a,4] and 4 nm.[19] It may also be pointed out here that the SPR peak positions are mainly influenced by size and shape[20] and refractive index of the embedding medium.[8] The matrix refractive index (n) of the TL film heated at 500 °C is 1.411 (at 550 nm) and we may expect that this value will remain more or less similar after heat treatment at 550 °C. If the value of n at all increases due to heat treatment at 550 °C, the SPR would have to be shifted to a higher wavelength.[14] It is also known that the SPR absorption position has a little effect if the diameter of the nanoparticles remains within 20 nm.[14] On the contrary, the fwhm has a pronounced effect on the size of the nanoparticles[14,17] and we indeed observed a decrease of fwhm due to an increase of particle diameter with respect to the heat-treatment temperatures. So the blue-shifting of SPR observed during heat treatment is mainly due to the progressive increase of Ag content in the Au−Ag alloy nanoparticles. Accordingly, the x_{Au} present in the alloy (see Table 2) is found to be about 0.81 after heat treatment at 450 °C (alloy SPR at 504 nm) and this value reaches about 0.50 after heat treatment at 550 °C for 2 h (alloy SPR at 468 nm).[21]

3.2. FTIR Spectra. Figure 3 shows the FTIR spectra of dried and UV/thermal-treated films showing the peak assignments and positions. The first layer, i.e., Au-doped film dried at 60 °C (Figure 3, curve a), shows the presence of Si−O−Si (asymmetric stretch) overlapping with Si−O−C at around 1090 cm^{-1}, Si−OH at 942 cm^{-1},[6a,22] Si−O−Si (symmetric stretch) at 795 cm^{-1} and 448 cm^{-1}.[6a,22] All these peaks remain unaltered after deposition of the Ag layer onto the Au layer and subsequently dried at 60 °C; however, as expected, intensities of all peaks become almost double due to the presence of two layers (Figure 3, curve b). The absence of any peak at 1385 cm^{-1} for NO_3^- vibration[11] indicates complete decomposition of $AgNO_3$. No significant change in the FTIR spectrum is observed after UV treatment of the TL films (Figure 3, curve c). The above spectra (Figure 3, curves a−c) also show the presence of organic peaks due to

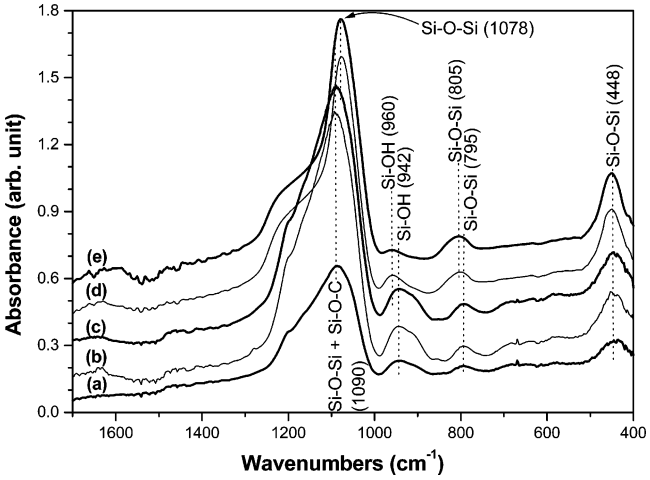

Figure 3. FTIR spectral evolution after deposition of (a) Au-doped film (first layer) dried at 60 °C, (b) Ag-doped film onto the first layer and dried at 60 °C, (c) after UV treatment (2.75 J/cm^2) of the two-layer (TL) film assembly using a conveyorized UV-curing machine and after heat-treatment at (d) 450 °C for 1 h and (e) 550 °C for 2 h. Films were deposited on double-side polished (intrinsic, IR transparent) Si wafers.

C−H vibrations in the regions 2870−2950 cm^{-1} and 1400−1500 cm^{-1} and epoxy vibration at 910 cm^{-1}. After heat treatment of the films at 450 °C, all such organic peaks vanished; the Si−O−Si (asymmetric stretch) peak shifted toward lower wavenumbers whereas the Si−OH and Si−O−Si (symmetric stretch) peaks are shifted toward higher wavenumbers (Figure 3, curve d). The shifting of Si−O−Si (asymmetric stretch) toward lower wavenumbers (1078 cm^{-1}) indicates the presence of porosity in the silica network after elimination of organics.[23] Low refractive index (1.411) value of the heat-treated film compared to the dense silica (1.46) also supports this. Heat treatment of the films to 550 °C caused further silanol (Si−OH) condensations and, as a result, Si−OH peak with reduced intensity has been observed (Figure 3, curve e).

3.3. XRD. As silver and gold have very similar lattice parameters of 0.408 and 0.409 nm,[3b,24] it is difficult to distinguish them by XRD or electron diffraction (TEM). The presence of nanoparticles can however be detected from XRD and TEM studies. Figure 4 shows XRD spectra of the dried and UV/thermal-treated TL films. TL film dried at 60 °C shows a weak peak at $2\Theta = 38.2°$ due to Au/Ag (111) reflections (Figure 4, curve a). This, along with the observation of Au- and Ag-SPR in the UV−visible spectra, confirm the presence of some Au and Ag separated nanoparticles in the film after drying at 60 °C. After UV treatment, the Au/Ag reflection is intensified (Figure 4, curve b), indicating formation of more separated Au and Ag nanoparticles, which is also supported by the presence of intense Au- and Ag-SPR peaks in the respective UV−visible spectra (Figure 1, curve c). In this case we also observe XRD peak at $2\Theta = 32.3°$ (Figure 4, curve b) due to the presence of some AgCl crystallites.[10,25] So UV treatment could not reduce all AgCl that formed due to the reaction of $AuCl_4^-$ and $AgNO_3$. However, after heat treatment at 450 °C and above (Figure

(19) Han, S. W.; Kim, Y.; Kim, K. *J. Colloid Interface Sci*. **1998**, *208*, 272.
(20) Jin, R.; Cao, Y.-W.; Mirkin, C. A.; Kelly, K. L.; Schatz, G. C.; Zheng, J. G. *Science* **2001**, *294*, 1901.
(21) We also verified the Au−Ag alloy formation in another two-layer film comprising successive overlapping layers approximately equal in thickness with 4 mol % Au-doped (first layer) and 2 mol % Ag-doped sols. This TL film assembly is expected to form Au−Ag alloy of approximate molar ratio 2:1 after UV/thermal treatment. As expected, after drying and UV and heat treatment at 550 °C for 2 h the film shows Au−Ag alloy SPR at 482 nm, which matches with the alloy composition of $Au_{0.62}Ag_{0.38}$,[3f] close to that of nominal value $Au_{0.66}Ag_{0.33}$.
(22) Medda, S. K.; Kundu, D.; De, G. *J. Non-Cryst. Solids* **2003**, *318*, 149.
(23) De, G.; Kundu, D.; Karmakar, B.; Ganguli, D. *J. Non-Cryst. Solids* **1993**, *155*, 253.
(24) Kittel, C. *Introduction to Solid State Physics*; Wiley: New York, 1996.
(25) Tomonaga, H.; Morimoto, T. *Thin Solid Films* **2001**, *392*, 355.

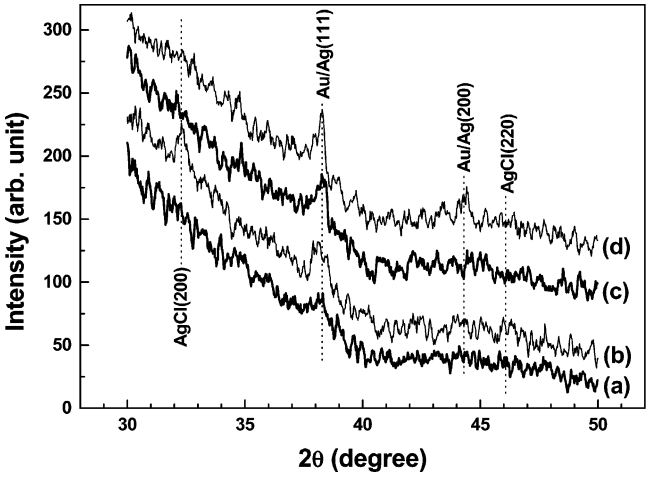

Figure 4. X-ray diffraction spectra of the TL films: (a) dried at 60 °C, (b) UV-treated (2.75 J/cm^2) and heat-treated at (c) 450 °C for 1 h and (d) 550 °C for 2 h.

4, curves c and d) we did not observe any AgCl peak, confirming the decomposition of residual amount of AgCl.[10,24] In the later cases XRD peaks related to the Au−Ag alloy nanoparticles only are observed, which is also confirmed by the appearance of Au−Ag alloy SPR absorption band between the Au- and Ag-SPR positions.[3,4,12]

3.4. TEM. Figure 5 shows TEM of two representative TL film samples heated at 450 °C for 1 h and 550 °C for 2 h, which are showing SPR bands at 504 and 468 nm, respectively (Table 2, Figure 2). The 450 °C heated sample shows the presence of spherical Au−Ag alloy nanoparticles ($x_{Au} \approx 0.8$) of average diameter ($\langle D \rangle$) 2.5 nm (Figure 5a−c) with uniform size distribution. The high-resolution image presented in Figure 5b shows characteristic lattice fringes of the embedded alloy nanoparticles. TEM of the 550 °C heated sample shows relatively larger alloy nanoparticles ($x_{Au} \approx 0.5$) of $\langle D \rangle$ 4.5 nm (Figure 5d−f). In this case also the high-resolution image shows clear lattice fringes (Figure 5e). It is therefore clear from TEM studies that upon increasing the heat-treatment temperature the size of the nanoparticles are increased. The corresponding UV−visible spectra also support the TEM observation (Figure 2) showing a decrease of fwhm of the SPR absorption band (Table 2) upon increasing heat-treatment temperature from 450−550 °C. Therefore, an increase of heat-treatment temperature not only increases Ag content in the alloy but also increases the size of the alloy nanoparticles. So the UV−visible spectral result corroborates well with the TEM observation. In an earlier work[8] we observe the formation of larger Au nanoparticles of about 20 nm in diameter in a similar SiO_2 host after heat treatment at 500 °C. However, in the present case the size of alloy nanoparticles are found to decrease drastically ($\langle D \rangle$ at 450 and 550 °C are 2.5 and 4.5 nm, respectively) and also showed uniform distributions. Large fwhm of alloy SPR absorption bands as well as TEM observation confirmed this.

As pointed out earlier the gold and silver have similar lattice parameters and from the known fact of their alloy formation in the bulk phase[26] it is expected that, in the present case, complete alloy formation takes place easily when they come into contact by diffusion during thermal annealing. The

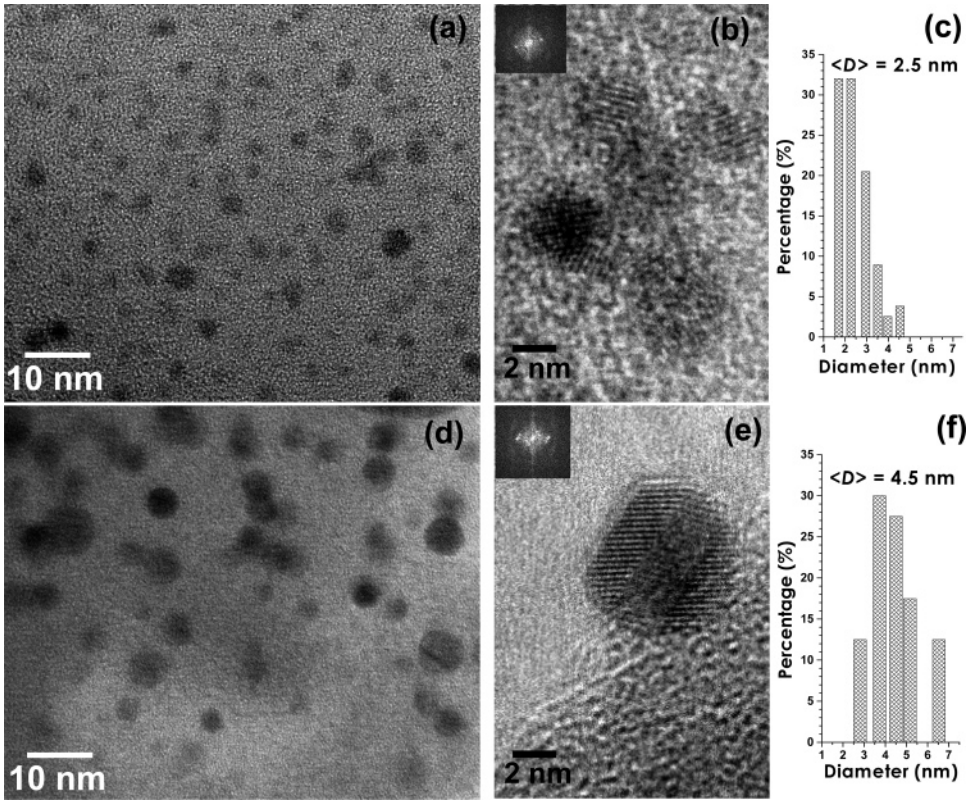

Figure 5. Transmission electron microscopy (TEM) images showing Au−Ag alloy nanoparticles embedded in TL films heated at 450 °C for 1 h (SPR at 504 nm; see Figure 2, curve a) and 550 °C for 2 h (SPR at 468 nm; see Figure 2, curve d): (a) TEM image of 450 °C film, (b) corresponding high-resolution image with Fourier diffractogram (inset), and (c) size distributions obtained from (a); (d) TEM image of 550 °C film, (e) corresponding high-resolution image with Fourier diffractogram (inset), and (f) size distributions obtained from (d).

two-layer coating assembly should not have any interface problem (similar matrix) for interlayer diffusion. Earlier work[16,27] showed that the diffusion of Ag in glassy SiO_2 would be more favorable than Au during thermal annealing in air. In a previous work[16] we observed that the diffusion of Ag nanoparticle occurred in SiO_2 film well below its melting temperature in air, causing loss of Ag from the film. The oxidizing atmosphere (air) causes oxidation of Ag and favors its migration in SiO_2. Although gold has a very weak affinity for oxygen,[28] oxygen-assisted gold diffusion and aggregation in SiO_2 was reported.[5a,29] In our TL coating system many separated Au and Ag nanoparticles were formed after UV treatment. When this UV-treated TL film is heated in air, oxidation of Ag would occur (supported by the fact that the Ag-SPR appeared after UV treatment of Ag-doped film and disappeared after heat treatment in air; see section 3.1), favoring its diffusion in the SiO_2 film. It is also noteworthy that the melting temperature of nanoparticles varies with the size; the smaller the particle, the lower the temperature. The melting point of a Au particle with size approximately 2 nm is estimated to be lower than 300 °C.[28] Since the size of nanoparticles formed in the present study are very small (<2 to ~5 nm), it is expected that these nanoparticles would remain in an active molten state at the temperature 450−550 °C.[28] So we may conclude that the Au−Ag alloy formation would occur through the interlayer diffusion of such molten Au and Ag nanoparticles to each other (the diffusion of Ag would be favorable because of oxidation) in such relatively porous two-layer SiO_2 film during thermal annealing in air. In the first stage of heat treatment (450 °C) Au nanoparticles (whose formation was complete at this stage) form alloy with a part of Ag (about 19% of total) and the major part of Ag remains as oxidized species.[18] With further increase in temperature, more and more oxidized Ag combines with Au, resulting in the formation of Au−Ag alloy, and after heat treatment at 550 °C for 2 h complete alloy formation ($Au_{0.5}Ag_{0.5}$) occurred.

Conclusions

Our result shows that using two successive overlapping sol−gel coating layers containing Au and Ag ions, respectively, followed by UV/thermal annealing, the formation of Au−Ag alloy and its composition could be controlled easily and systematically by controlling simply the annealing temperature in air. Formation of Au−Ag alloy nanoparticles of uniform size distributions ($\langle D \rangle \approx 2.5-4.5$ nm) inside a glassy SiO_2 film matrix with desirable alloy composition and SPR absorption positions between Au- and Ag-SPR is noteworthy and could be of potential technological interest for optical switching applications using lasers of different wavelengths.

Preliminary observation shows that this new TL strategy also works well in preparing other bimetallic alloy nanoparticle doped coatings. The results will be reported in subsequent communications.

Acknowledgment. Financial support from the Department of Science and Technology (DST), Government of India, in the form of a project (SR/S5/NM-13/2002) under the '*Nanomaterials Science and Technology Initiative*' (NSTI) program is thankfully acknowledged. The authors thank Dr. H. S. Maiti, Director, CG&CRI, for his kind permission to publish this work.

CM051572R

(26) Okamoto, H.; Massalski, T. B. *Phase Diagrams of Binary Gold Alloys*; ASM International: Metals Park, OH, 1987.
(27) Vosburgh, J.; Doremus, R. H. *J. Non-Cryst. Solids* **2004**, *349*, 309.
(28) Buffat, Ph; Borel, J.-P. *Phys. Rev. A* **1976**, *13*, 2287.
(29) Battaglin, G.; Cattaruzza, E.; Gonella, F.; Mattei, G.; Mazzoldi, P.; Sada, C.; Zhang, X. *Nucl. Instr. Methods Phys. Res., Sect. B* **2000**, *166*, 857.